We are IntechOpen, the world's leading publisher of Open Access books Built by scientists, for scientists

4,800
Open access books available

122,000
International authors and editors

135M
Downloads

Our authors are among the

154
Countries delivered to

TOP 1%
most cited scientists

12.2%
Contributors from top 500 universities

CLARIVATE ANALYTICS BOOK CITATION INDEX INDEXED

WEB OF SCIENCE™

Selection of our books indexed in the Book Citation Index in Web of Science™ Core Collection (BKCI)

Interested in publishing with us?
Contact book.department@intechopen.com

Numbers displayed above are based on latest data collected.
For more information visit www.intechopen.com

Chapter 2

Silicon Solar Cells with Nanoporous Silicon Layer

Tayyar Dzhafarov

Additional information is available at the end of the chapter

http://dx.doi.org/10.5772/51593

1. Introduction

Today's photovoltaic solar panels are widely used to supply the power and buildings. The account of total solar cell product in 2010 was about 20 GW. Over 95% of all solar cells produced world wide are composed of the silicon (single crystal, polycrystalline, amorphous, ribbon etc.) and domination of silicon-based solar cell market probably will be do so in the immediate future. The main reason for dominant role of silicon solar cells in word market is high quality silicon that produced in large quantities for microelectronic industry. Additionally silicon solar cell processing does not burden the environment.

The main requirements for ideal solar cell material are (a) direct band structure, (b) band gap between 1.1 and 1.7 eV, (c) consisting of readily available and non-toxic materials, (d) good photovoltaic conversion efficiency, (e) long-term stability [1]. Silicon is the second most abundant element in the earth's crust (35 %) after oxygen. It is the base material for photovoltaic conversion of solar spectrum radiation ranging from ultraviolet to the near infrared, however it can absorb the small portion of solar radiation, i.e. can convert photons with energy of the silicon band gap. The theoretical curve for conversion efficiency of solar cell materials versus band gap for single junction cell (Figure 1) shows that silicon (1.1 eV) is not at the maximum of the curve (about 1.4-1.5 eV) but relatively close to it [2]. The efficiency for ideal silicon solar cell can reach about 30% (for AM1.5 at 300K).

Photoelectron properties related with indirect band structure and high reflectance of crystalline silicon (about of 30-35%) are still a challenger for creation solar cells with high conversion efficiency. High refractive index of crystalline silicon (about 3.5) in solar spectrum

region of 300-1100 nm creates large optical losses which can be reduced by using antireflection coating (ARC). Although highly efficient double and triple antireflection coatings are available, most manufactured crystalline silicon solar cells employ simple and inexpensive single-layer ARC with relatively poor antireflection properties.

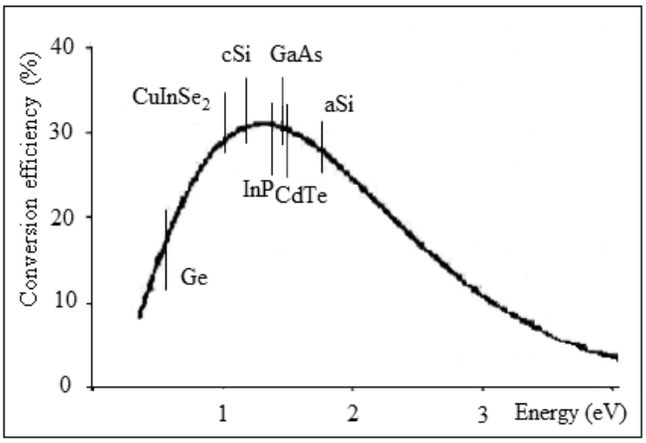

Figure 1. Conversion efficiency depending on semiconductor band gap (AM1.5, 300K).

The first observation of a visible photoluminescence at room temperature in nanostructured porous silicon opened the possibilities of wide range photonic and biologic applications due to tunable refractive index, large surface/volume ratio an biocompatibility of porous silicon [3]. Today the porous silicon is quickly becoming very import and versatile material for solar cell technology.

The crystalline structure, chemical, electrical, photoluminescence and optical properties of porous silicon have been extensively studied by various experimental techniques [4]. Porous silicon can be formed by chemical etching, electrochemical etching and photo-electrochemical etching of silicon in HF-based solutions at room temperature. Therefore the chemical technology can be more adapted to industrial fabrication of solar cells due to its simplicity and lower cost. Porosity, thickness, refractive index of layer, pore size etc. depend on formation parameters (electrolytes contents, current density, temperature, crystal orientation, doping type and concentration, time etching etc.). Sizes of pore and pores walls can be varied from 5-10 nm to hundreds micrometers dependent on fabrication parameters. Possibilities of minimization of reflectance (due to light trapping in pores), increase of band gap of porous silicon layer (due to quantum confinement of charges in the PS microcrystallites) by changing of porosity allow to use PS layer as both ARC and wide-band gap photosensitive layer. Last years the porous silicon layers are widely used in silicon solar cell applications.

This chapter has focused on review of investigations concerning using of porous silicon layers in silicon solar cells and also characterization of structure and properties of porous layers.

http://dx.doi.org/10.5772/51593

2. Photovoltaic characteristics of solar cells

For the solar cell with the series resistance R_s and shunt (or parallel) resistance R_{sh} current-voltage characteristic is determined as [5]

$$I = I_0\left\{\exp\frac{qV - IR_s}{AkT} - 1\right\} + \frac{V - IR_s}{R_{sh}} - I_l \tag{1}$$

Here I_o is the reverse saturation current, A is diode ideality factor, q is elementary charge, k is Boltzmann's constant, T is absolute temperature, I_l is photo-generated current. Figure 2 shows the representation of the dark and the illuminated characteristics of the *p-n* junction.

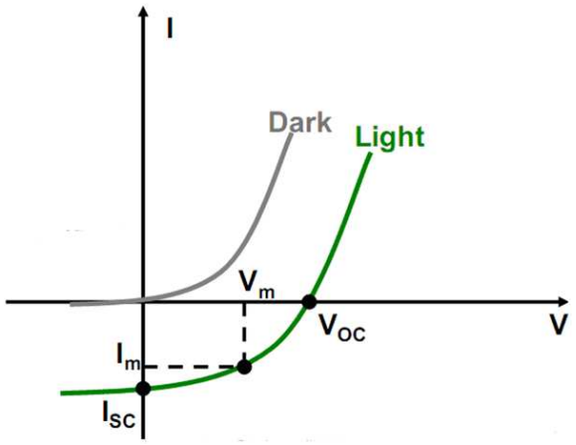

Figure 2. The dark and light current-voltage characteristics of the *p-n* junction.

The reverse saturation current is given

$$I_0 = \frac{qD_n n_i^2}{L_n N_A} + \frac{qD_p n_i^2}{L_p N_D} \tag{2}$$

Here L_n and L_p are diffusion length, D_n and D_p are diffusion coefficient of minority carriers (electrons and holes, respectively), n_i is intrinsic carrier concentration, N_A and N_d are concentration of acceptor and donor impurities, respectively.

When the solar cell is operated at open circuit (I=0, i.e. the shunt resistance is high) then the open-circuit voltage is give

$$V_{OC} = \frac{AkT}{q}\ln\left(\frac{I_l}{I_0} + 1\right) \approx \frac{AkT}{q}\ln\frac{I_l}{I_0} \tag{3}$$

Very low values of R_{sh} produces a significant reduction of V_{oc}. An increase in reverse saturation current I_o produces a reduction in V_{oc}. The reverse saturation current is determined by

the leakage current of carriers across the *p-n* junction under reverse bias. The leakage current is a result of recombination of carriers on either side of the junction. For the solar cell working at short circuit (V=0, i.e. low R_s and I_o, and high R_{sh}) the short-circuit current is equal to photocurrent $I_{sc} \approx I_l$.

The series resistance of cell depends on concentration of carriers in *n*- and *p*-region, depth of *p-n* junction, resistance and construction of frontal and back ohmic contacts. Increase of series resistance produces a significant reduction in I_{sc}.

The conversion efficiency of the solar cell is defined as the percentage of incident of solar power, which the can convert in electrical power

$$\eta = \frac{P_m}{E_l S} \tag{4}$$

Here $P_m = I_m V_m$ (in Watt) is maximum electrical power, I_m and V_m values of current and voltage corresponding the maximum output power (Fig. 2), E_l (in W/m^2) is light irradiance and S is the surface area of the solar cell.

The fill factor (FF) defines the portion of electrical power produced in solar cell in load. The fill factor is the ratio of the maximum electrical power divided by the open-circuit voltage and the short-circuit current

$$FF = \frac{P_m}{I_{sc} V_{oc}} = \frac{I_m V_m}{I_{sc} V_{oc}} \tag{5}$$

Substituting P_m from Eq.(4) in Eq. (5) gives for the efficiency

$$\eta = \frac{V_{oc} I_{sc}}{E_l S} FF \tag{6}$$

The series and shunt resistance of solar cell influence on the fill factor. Increase of shunt resistance and decrease of series resistance result in to higher fill factor and thereby to larger efficiency.

For crystalline silicon solar cells efficiency about 25% in laboratory and 14% commercially is reached. A theoretical limit of efficiency of crystalline solar cell is about 30%. Comparison efficiency of industrially produced silicon solar cells with theoretical efficiency shows that about 85% power losses occur in commercially cells.

The present efficiency and cost of the silicon solar cell in comparison with conventional energy sources limit the wider using of silicon cells. To improve the performance of solar cells, the power losses must be reduced. The maximum absorption (i.e. minimum reflectance), minimum recombination and series resistance are most conditions for reaching a high efficiency solar cell. The reduction of different energy losses in crystalline silicon solar cells is the most problem of improvement of the conversion efficiency and thereby of reduction of cost.

http://dx.doi.org/10.5772/51593

3. Losses in solar cells

The losses in silicon solar cells can be related with: (a) recombination losses, (b) series resistance losses, (c) thermal losses, (d) metal/semiconductor contact losses,(e) reflection losses [6].

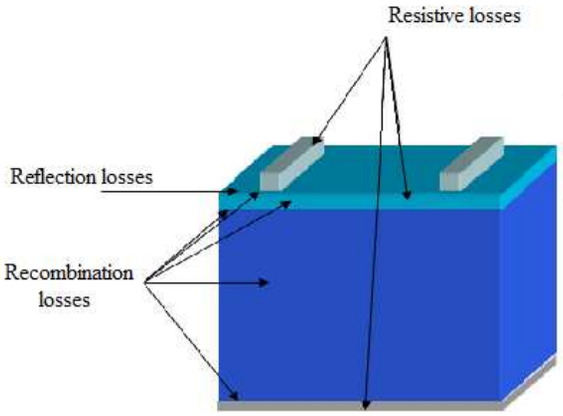

Figure 3. Schematic representation of energy losses in solar cell.

(a) Recombination losses can be caused as result of surface and bulk recombination, recombination in depletion region and recombination at metal/semiconductor contact (Figure 3). Recombination losses mainly influence on the open-circuit voltage.

The incomplete chemical bonds presenting on the surface of semiconductor play role of traps for photo-excited carriers and therefore recombination on traps can result in reduction on photocurrent. The surface recombination velocity S is expressed as

$$S = \sigma v N_t \tag{7}$$

Where σ and v are capture cross section for carriers and thermal velocity of carriers, respectively, N_t is the number of surface traps. The decrease of surface recombination velocity is usually reached by deposition of thin passivation films on top surface of cell (for example SiO_2 or Si_3N_4 films) by chemical vapor deposition (CVD), plasma enhance chemical vapor deposition (PECVD) or thermal oxidation technique). The standard technique for the reduction of the surface state density of Si is thermal oxidation at 800°C for 15 min in dry oxygen [7]. Passivation of silicon surface results in significant reduction of surface recombination velocity (from $8x10^4$ to $1.6x10^2$ cm/s).

Impurities and crystalline defects, presenting in bulk region of semiconductor can play role of traps for carriers. Reduction of concentration of rest impurities in bulk of semiconductor, according to Schockey and Read model, will decrease the trap-assisted recombination velocity. Using the bulk semiconductor material having lower concentration impurities and defects can increase the diffusion length of minority carriers and thereby can decrease the recombination losses in bulk of solar cells.

(b) Series resistance of a solar cell consists of several components, such as top grid and busbar resistance, emitter resistance; semiconductor bulk resistance and metal/semiconductor

contact resistance (see Figure 3). The series resistance controlled by the top contact design and emitter resistance must be carefully designed for each type of solar cell in order to optimize efficiency of solar cell. The semiconductor bulk resistance is low (about 10^{-3} Ω) due to its high conductivity. High values of series resistance will produce a significant reduction in short-circuit current. Losses caused by series resistance are given by $P = V_{Rs}I = I^2R_s$ and increase quadratic with photocurrent and therefore they most important at high illumination intensities. Very low values of shunt resistance R_{sh} will produce a significant reduction in open-circuit voltage. A low shunt resistance is a processing defect rather than a design parameter. Both series and shunt resistance losses decrease the fill factor and efficiency of a solar cell.

The characteristic equation for solar cell described by Eq. (3) shows that an increase in reverse saturation current I_o produces a reduction in open-circuit voltage. Increase of reverse saturation current means rising of leakage of carriers across the *p-n* junction under reverse bias due to recombination of carriers in depletion regions on either side of junctions. Recombination proceeding in the depletion regions is less significant as compared to the surface recombination due to the electrical field of *p-n* junction that separates the photo-generated electrons and holes.

Reduction of emitter layer resistance is reached by optimization of the doping concentration of layer and the *p-n* junction depth. For (n^+-*p*) silicon solar cell the optimal values of junction thickness and doping concentration about of $d_{pn} \approx 0.8$ μm and $n^+ \approx 2 \times 10^{19}$ cm^{-3} respectively.

(c) Thermal losses consist of a significant portion of losses in photovoltaic solar cells. The excess energy formed at absorption of the solar photons that is larger than the band gap energy of semiconductor is realized in the form heat. The temperature rise of solar cell results in increase in the reverse saturation current I_o due to an increase concentration of the intrinsic carriers n_i and diffusion length of minority carriers (Eq. (2)). The increase in reverse saturation current reduces the open-circuit voltage (Eq. (3)). Increase in I_o means the rising the "leakage" of carriers across the *p-n* junction under reverse bias due to recombination of carriers in the neutral regions on neither side of the junction.

(d) Metal/semiconductor contacts placed on the frontal and back surfaces of solar cell cause considerable losses. The screen-printed technique is often used for deposition metallic contacts to silicon solar cells[8]. The frontal contact has form of fine grid lines and the back contact is a metal plate covering entire back surface of cell. Ag and Ag-Al pastes are used in conventional silicon solar cells by deposition of frontal and back ohmic contacts by screen-printed technique. Reduction of resistance of metal/semiconductor contacts is one of major means decrease of power losses for cells. Presence of acceptor type impurity (Al) in back contact (Ag-Al) results in decrease the resistance of near-back contact region of *p*-type silicon substrate due to diffusion penetration of aluminum during thermal treatment. Moreover, the heavy doping forms the near-surface electric field that reduces the recombination losses at metal/semiconductor contact.

(e) Reflection losses. A large portion of energy losses during solar cell operation could be attributed to optical losses caused by large value of reflectance (about 35%) in the spectral

range where silicon is photosensitive [9]. Traditional techniques of texturing and antireflection coating (ARC) have been applied widely to decrease the reflectance of silicon surface. This technology is most used in industrial production of silicon solar cells [10]. The texturisation adds micrometer-scale tilted pyramid structure to the silicon surface, which reduces reflection of the incident light (Figure 4) [11].

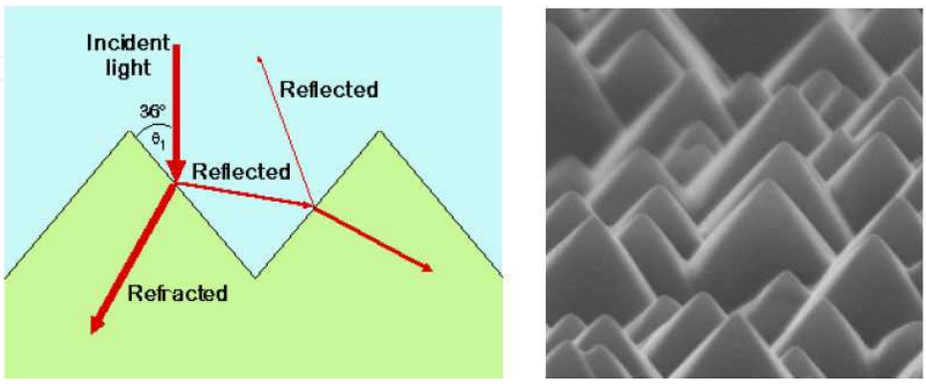

Figure 4. The schematic representation of multiple light reflection (on left) and optical microscopy image of textured silicon surface (on right).

Pyramids are usually formed by etching the surface with acid (H_2SO_4, HNO_3:H_2O etc.) or with alkaline etch (NaOH, KOH etc.). The light bouncing from pyramid to pyramid increases the optical path and increases absorption of visible light in silicon, thus increasing the efficiency of solar cell. Antireflection coating presents thin film of a transparency material with refractive index (n) between those of air (n_o=1) and silicon (n_{Si} = 3.84). ARC reduces the Fresnel reflection caused from light penetration from a medium of one refractive index to another (for example air/semiconductor).

The optimization of parameters (the refractive index and thickness) of ARC was based on the stratified medium theory and Bruggeman effective medium approximation [12]. The zero-reflection for normal incidence of light on ARC/Si system is given [13]

$$n_{arc} = (n_o n_{Si})^{1/2} \tag{8}$$

Here $n_{arc,}$ $n_o$and $n_{Si}$are the refractive indexes of antireflection coating, the ambient media (air) and silicon, respectively.

The optimal single-layer ARC (SLARC) thickness (d_{arc}) for minimum reflection for wavelength λ is given [14]

$$d_{arc} = \lambda / 4n_{arc} \tag{9}$$

If conditions (8) and (9) for air/SLARC/Si system are to be satisfied (n_o = 1, n_{Si} = 3.84), then the optimal values of refractive index and thickness (a quarter of wavelength) of SLARC must be (for λ=650 nm) n_{arc}= 1.96 and d_{arc}=80 nm. For glass/SLARC/Si system (where a glass is protecting layer) optimal values for n_{arc} = 1.55 and d_{arc}= 65 nm.

For double-layer antireflection coating (DLARC) with refractive index of top and bottom layers n_1 and n_2, respectively, on silicon (air/ARC(top)/ARC(bottom)/Si system) the zero-reflectance at normal incident light is realized at conditions [15]

$$n_1 = (n_o n_2)^{1/2} \quad \text{and} \quad n_2 = (n_1 n_{Si})^{1/2} \tag{10}$$

Here n_1 and n_2 are refractive index of top layer 1 and bottom layer 2, respectively. For air/layer 1/layer 2/Si system, the ideal values for top layer are n_1= 1.57 and d_1 = 102 nm, whereas the bottom layer parameters are n_2 = 2.46 and d_2 = 65 nm.

Different types of SLARC (SiO_2, ZnS, Al_2O_3, Ta_2O_3), DLARC (MgF_2/ZnS, SiO_2/TiO_2, MgF_2/TiO_2, MgF_2/CeO_2, SiO_2/SiH etc.) and multilayer ARCs are used for reduction for reflectance of silicon solar cells. Optimal values refractive index and thickness for single-layer ARCs on silicon surface (air/ARC/Si system, for λ = 650 nm) are presented in Table 1.

ARCs	n_{arc}	d_{arc} (nm)
SiO_2	1.4	116
Si_3N_4	2	81
ZnS	2.25	72
ZnO	2	81
MgF_2	1.4	116
TiO_2	2.5	65
SnO_2	1.9	86
SiN_x:H	1.9-2.4	68-86
Por.Si	(1.2-2.2)*	74-135

* For porosity from 52% to 80%

Table 1. Optimal values of refractive index and thickness of the single-layer ARCs on silicon.

As stated above ARCs are generally fabricated by chemical vapor deposition, plasma-enhanced chemical deposition, thermal oxidation processes. They are carried out at high temperatures resulting in an increase in the cost of solar cells [16]. Traditional antireflection coating and surface texturing may reduce reflection efficiently (up to 10-15%) at low wavelength in the visible spectrum (about 400-800 nm), but they are less efficient at harvesting light in the near infrared spectrum (more than 800 nm). The significant of portion of solar radiation, penetrating through the atmosphere, lies at wavelength greater than 800 nm, therefore solar cells with traditional ARC and surface textures leave a huge amount of potential energy out of the using.

Use the single layer ARCs is most simple, low cost and suitable for silicon solar cell technology as compared to expensive and impractical double- or multilayer ARCs. A single layer ARC allows a reduction of reflectance (up to 11%) only in a narrow wavelength range of so-

http://dx.doi.org/10.5772/51593

lar spectrum. A single-layer coating cannot reduce the reflection in a wide wavelength because of neighboring interference maxima. A wider spectral range may be obtained either by increasing the number of layers or by using an inhomogeneous layer with gradient of refractive index. Usage of such inhomogeneous layer allows to suppress the interference maxima narrowing the spectral range. Using the ARC with monotonous changeof the refractive index on the depth can raise the performance of silicon solar cells. ARCs with a graded refractive index constituted from silicon and titanium oxides mixtures were studied in [17]. 3.7% average reflectance between wavelength from 300 to 1100 nm and 48% improvement of the photocurrent was reached on using silicon and titanium oxides mixtures as graded ARC on silicon. It is believed that the porous silicon with tunable refractive index can be adapted production of silicon solar cells due to the simple and cheap technology.

4. Fabrication and Properties of Porous Silicon

Porous silicon layer on monocrystalline Si substrate and its manufacture by the technique of electrochemical etching of silicon substrate in HF solution or by chemical etching in HF-HNO_3 mixture are known as early as from 1956 [3,18]. Electrochemical etching of silicon is attractive because of the possibility to tune the pore size from a few nanometers to a few tens of micrometers, just by choosing wafer doping level and etching conditions. Moreover, a wide range of porous layer thickness, porosities, surface areas and morphologies can be formed depending on the etching conditions. The bulk silicon was shown modifies during the etching to sponge-like structure with silicon columns and hydrogen covered pores.

The simplest electrochemical cell is shown in Figure 5. The Si wafer acts as the anode and the platinum is the cathode. The thickness of porous silicon layer on Si substrate is determined by duration of etching. The porosity, i.e. the void fraction in the porous layer is determined by the current density (about 10 - 100 mA/cm^2), composition electrolyte, resistance and the doping density of Si substrate.

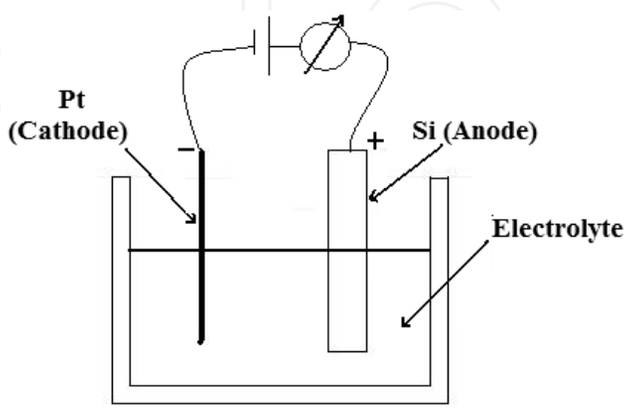

Figure 5. Cross-sectional view of lateral anodization cell.

The anodic reaction on the Si substrate can be written during pore formation as [19]

$$Si + 6HF \rightarrow H_2SiF_6 + H_2 + 2H^+ + 2e^- \quad (11)$$

Silicon atoms are dissolved as SiF_6^{2-} require the presence of F^- ions (from HF solution) and positively charges holes (from the silicon wafer) at the silicon interface. Concentration of holes in *p*-Si is sufficiently high (about 10^{14} - 10^{18} cm^{-3}) and this case the nano-size pores were formed. Concentration of holes in *n*-Si is very small (about 10^2-10^6 cm^{-3}) and therefore generation of holes is possible due to illumination of *n*-Si substrate.

The porous silicon layers are often prepared in composition of HF:H_2O, HF:C_2H_5OH, HF:C_2H_5OH:H_2O, HF:HNO_3, HF:HNO_3:H_2O. Fabrication of porous silicon layers on *n*-type silicon substrates is usually produced under illumination. Before the etching process the silicon substrate are dipped in HF:H_2O (1:50) solution for remove the native oxide film on silicon surface.

The structure and size of pores in porous silicon layer formed on *n*-Si substrate differ from those for layer on *p*-Si. If electrochemical etching was carried out at relatively low current density (10-80 mA/cm^2), then the local dissolution of silicon surface takes place. Herewith, pore formation begins on surface defects of Si and further growth of pores into silicon substrate proceeds due to the holes diffusion to Si-electrolyte interface. In the case of large current density (0.5 - 0.8 A/cm^2) when the amount of holes moving to Si-electrolyte interface is very high, the etching of top regions of Si substrate is preferred. It ensures the uniform etching of silicon surface and formation a smooth surface of substrate (the so-called the electro-polishing process). The raising the current density above the critical value at the end of anodization process results in a detachment of the porous silicon film from Si substrates. The behavior at high current densities turns out to be useful to produce porous silicon free-standing layers. The anodic reaction during the electro-polishing can be written as

$$Si + 6HF \rightarrow H_2SiF_6 + 4H^+ + 4e^- \quad (12)$$

Pores, depending on the diameter, denoted as micropores (R < 2 nm), mesopores (2 nm < R < 50 nm) and macropores (R > 50 nm). Under illumination the pore size dependent on doping density and anodization conditions, with diameters in the range 100 nm - 20 μm (macropores).

The average porosity (*P*), i.e. the avoid fraction in the porous layer, can be obtained by gravimetric using the equation

$$P = \left\{ \frac{m_1 - m_2}{m_1 - m_3} \right\} 100(\%) \quad (13)$$

Here m_1 is Si sample mass before the anodization etching, m_2 just after etching and m_3 after the removal of the porous layer by electro-polishing or after a rapid dissolution of the whole porous layer in a 3% KOH solution. Guessing the porous silicon mass m_{PS}, the average porosity can be also determined by using the equation

http://dx.doi.org/10.5772/51593

$$P = \frac{1 - m_{PS}}{\rho s d} = \frac{m_1 - m_{ps}}{m_1} \tag{14}$$

One can also get the porous silicon layer thickness d using the equation

$$d = \frac{m_1 - m_3}{\rho S} \tag{15}$$

Here ρ is the Si density (2.33 g/cm^3) and S is the etched surface.

The inhomogeneity in porosity and thickness of porous of the porous layers is often observed on fabrication with electrochemical anodization cell. They are most probably due to the bubbles that form and stick on silicon surface. The inhomogeneity in porous and thickness must be removed and the concentration of the HF has to be locally constant on the surface of the silicon substrate. Removal of the bubbles on the surface of the silicon and thereby preparation of homogeneous porous silicon layers is realized with using a stirrer. The distance between the silicon wafer and the platinum cathode also influences on the homogeneity, whereas the shape of platinum cathode almost does not influence on homogeneity. There is a certain distance for given cell when the porous silicon layers are homogeneous.

The thickness of the porous silicon layers mainly depends on duration of anodization process, whereas the porosity depends on the current density. It is be noted that the character of the thickness-etching time and porosity-current density relations depend on orientation, type and concentration level in silicon and conditions anodization process (the electrolyte composition, distance between silicon wafer and platinum electrode, illumination etc.).

The thickness-etching time dependence for porous silicon layer fabricated on p-type (100) silicon substrates in 3HF:1C_2H_5OH solution at current density 20 mA/cm^2 is given in Figure 6 [20]. It is seen that the average growth kinetics of porous silicon layer is about 14 nm/s.

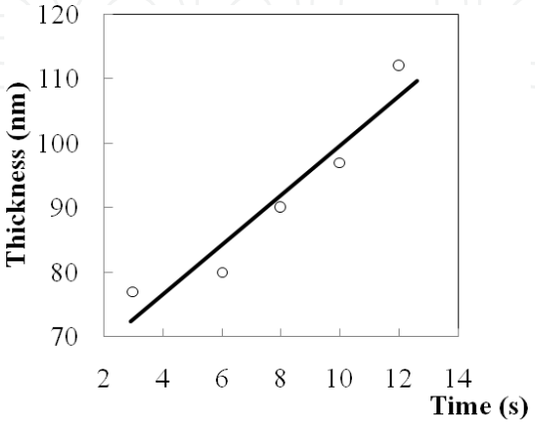

Figure 6. Thickness vs. etching time for porous silicon growth at constant current density of 20 mA/cm^2.

The porosity of the porous silicon layer almost linearly increases with the current density once the other etching parameters are kept fixed (Figure 7).

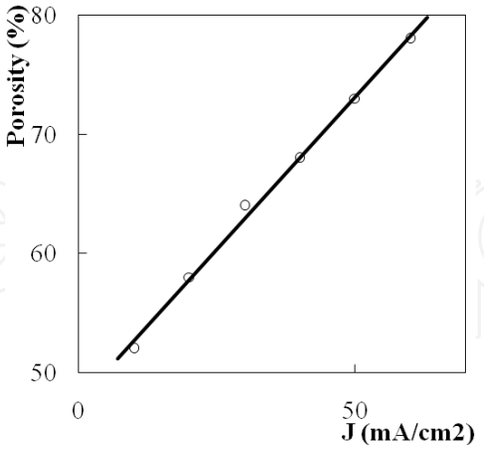

Figure 7. The porosity as a function of current density.

Porous silicon is a particular form of crystalline silicon. The crystalline structure of porous silicon presents a network of silicon in nano (micro)-sized regions surrounded by void space with a very large surface-to-volume ration (up to 10^3 m^2/cm^3) [13]. The structure of porous silicon is like a sponge or columnar where quantum confinement effects play fundamental role [4]. The pore surfaces are covered by silicon hydrides (Si-H) and silicon oxides (Si-O).

Figure 8 shows Fourier transform infrared (FTIR) spectrum of free-standing PS film of thickness of 12 μm measured at room temperature [21]. The peaks related with absorption on vibration of Si-H (2100 cm^{-1}) and Si-O bonds (1100 cm^{-1}) located on pore surfaces were observed from Figure 8. These bonds play an important role in regulating optical, electrical and gas sensing properties of porous silicon.

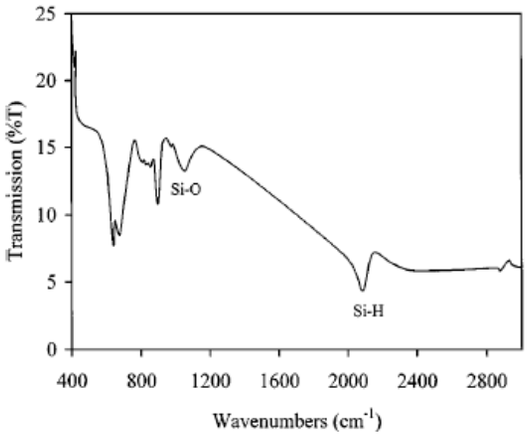

Figure 8. FTIR spectrum of porous silicon film (300 K).

The effect of isothermal annealing of free-standing PS films on changes of intensity of absorption coefficient of Si-H (2100 cm^{-1}) and Si-O (1100 cm^{-1}) peaks is used for estimation of diffusion coefficient [22]. Results of these measurements showed that in the range of 65-185°C the temperature dependence of hydrogen and oxygen diffusion coefficient along the porous surfaces are described as

http://dx.doi.org/10.5772/51593

$$D(H) = 5x10^{-10} \exp(-0.37\ eV/kT) \quad (16)$$

$$D(O) = 1.3x10^{-8} \exp(-0.50\ eV/kT) \quad (17)$$

The activation energy for diffusion of hydrogen along the porous surfaces estimated from response (or recovery) V_{oc} - t curves for Au/PS/Si cells under humid ambient (90%RH) is 0.34 eV [23].

The thermal oxidation of free-standing PS films in the range from 400 to 900°C is accompanied the structural phase transition [24]. The crystalline nanostructured silicon partly converts into amorphous and polycrystalline silicon, if temperature is about 500°C. At higher temperatures three Si structures (crystalline, polycrystalline and amorphous) produce SiO_2 (combination of cristobolite and quartz) due to the oxygen diffusion and absorption in PS. An optimal oxygen-absorption temperature is about 700°C.

The characterization of the lattice deformation of porous silicon carried out by X-ray diffraction has been described in [25, 26]. Crystalline structure of porous silicon layers is equivalent to that of nearly perfect silicon. Porous silicon may be considered as an assembly of small silicon crystallites. These crystallites have two different dimensions, the bigger one being oriented perpendicular to the surface. Typical values seem to be about 1000 Å and 10-100Å. Lattice parameter of the porous silicon of 54% porosity prepared on p^+-Si (100) substrate was slightly bigger (the difference (Δa) is $2.3x10^{-3}$ Å) than that of intrinsic silicon (a= 5.4306 Å).

A linear increase in the lattice parameter expansion (the lattice mismatch parameter Δa / a) for porous silicon going from 4 to $7x10^{-4}$ when the porosity increases from 34 to 72% has been measured [25]. The same behavior for lattice mismatch parameter (Δa / a)$x10^4$ between porous silicon layer and p^+-type silicon substrate depending on porosity has been found in [27].

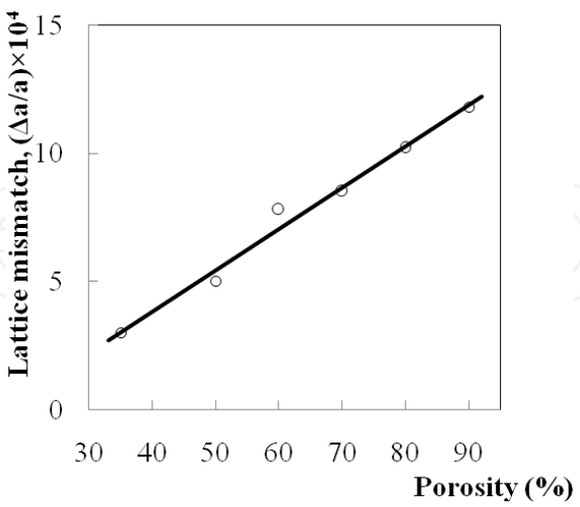

Figure 9. Relation for lattice mismatch parameter *Δa/a* between the PS layer and p^+-type Si substrate.

The origin expansion is attributed to the hydrogen-silicon bonds at the inner surface of the porous silicon. The hydrogen desorption results in a sharp contraction of the lattice parameter of porous silicon layer.

The pores on the surface of silicon increases absorption of light by increasing the effective thickness of emitter layer of solar cell (see Figure 4). Therefore the refractive index of the emitter layer, which strongly influences on efficiency of the solar cell depends on porosity of porous silicon. The current density applied during the formation process determines the porosity of the porous silicon layer and consequently its refractive index. We can say that the porosity-current density profile is transferred to the refractive index versus current density profile.

The reflectance can be calculated from refractive index. For film with parallel surfaces when light moves from a medium with refractive index n_1 to one with refractive index n_2 reflectance for normal incident is given as

$$R = (n_1 - n_2 / n_1 + n_2)^2 \tag{18}$$

The reflectance spectrum of the porous silicon film is characterized by the multiple interference fringes caused by the air-porous silicon and porous silicon-silicon interfaces. A simple method for evaluating the refractive index on a thin film is to measure the interference fringes resulting from multiple reflections

$$n = 1/2d\,(\lambda_1\lambda_2 \,/\, \lambda_2 - \lambda_1) \tag{19}$$

Here λ_1 and λ_2 are the wavelength for two consecutive maxima, d is the thickness of the film. The main advantage of this method determination of the refractive index is its rapidity and simplicity. This method has been used by different authors for normal incidence. Figure 10 illustrates the refractive index as a function of current density for low resistivity silicon substrate [28].

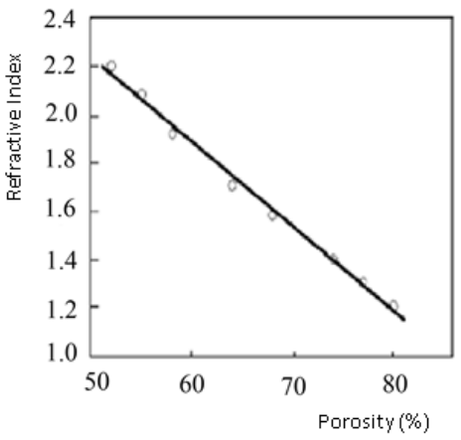

Figure 10. Refractive index as a function of current density for p^+-type doped substrate.

Three type of porous silicon layer with different refractive index profile along the thickness are used in solar cells as antireflection coating: *(a)* the refractive index is constant, *(b)* the refractive index profile smoothly changes, and *(c)* it changes in stepped form. The *(b)* type of porous silicon layer is fabricated by smooth change the current density during anodization process and *(c)* type porous silicon presents the multilayer structure which can be prepared by stepped variation of the current density during growth process.

http://dx.doi.org/10.5772/51593

As stated above the porous silicon consists of a network of nano-sized silicon walls and voids that formed when crystalline silicon wafer are etched electrochemically in HF-based electrolyte. Porous silicon presents the quantum system in which the charge carriers located in narrow crystalline silicon wall separating the pore walls. One of features of nanoporous silicon in comparison to the bulk silicon is shifting of fundamental absorption edge into the short wavelength of the visible region of the solar spectrum. It was confirmed by the measuring the optical absorption in the free-standing porous silicon layers [29].

PS layers with a thickness of 10-20 μm and an average porosity of 40 to 80% were prepared on *n*-type (111) Si substrates (ϱ =1×10^{-2} Ω cm) by anodic etching in HF:H_2O = 1:3 solution at a *dc* current of about 10-60 mA cm^{-2} under white-light illumination [30]. For optical and electrical measurements, the PS films were then detached from the Si substrate by electro- polishing in the same solution with a current density of 0.8-1.0 A cm^{-2}. The free-standing PS films were characterized by porosity, thickness, optical and resistance measurements. The average porosity was measured by a gravimetric technique. Resistance and charge carrier concentration measurements were carried out on the free-standing PS layers attached to a dielectric substrate (glass) by using the Van der Pauw technique.

Figure 11 shows the effective energy gap in dependency on porosity of the free- standing PS films, calculated from extrapolation of the high energy part of {α^2 ($h\nu$) ^{2}- $h\nu$} spectra [29]. Near linear increase of band gap from 1.4 to 1.9 eV with rising of porosity of PS films in the range of 30-90 % is observed.

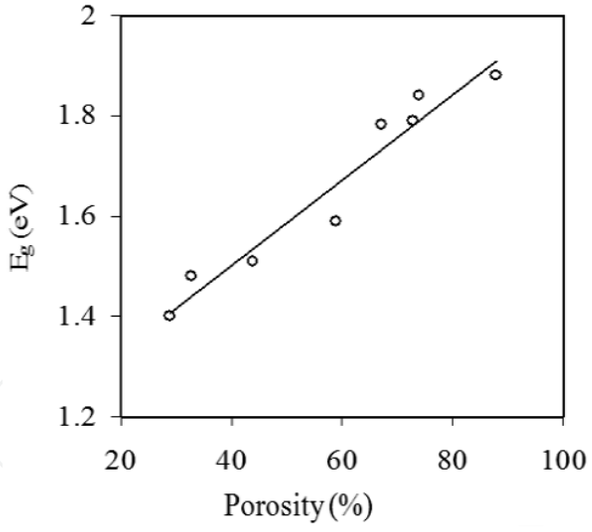

Figure 11. Energy band gap in depending on porosity of PS film (40% RH, 300 K).

Data on Figure 11 concerning increase of the energy gap in dependency on porosity of PS films can be explained by a model including the quantum confinement of carriers in the PS microcrystallites, causing the widening of the Si band gap.

The electrical measurements of the free-standing PS layers with 65% porosity (300 K, 45% RH) gave values of ϱ = 1.8×10^6 Ω cm for resistance, p = 9.6×10^{12} cm^{-3} for hole concentration, and μ = 0.36 cm^2/(V s) for hole mobility.

5. Porous silicon layers in silicon solar cells

As stated above the features of porous silicon (a quantum system, a sponge or columnar structure and an extremely large pore surfaces) provide many possible applications, such as light emitting diode, chemical and biological sensor, hydrogen fuel cell, photovoltaic cell, antireflection coating in solar cells etc.

Decrease of reflectance (between 30 and 3%) and increase of band gap of porous silicon layer (between 1.1 and 1.9eV) with increase of porosity makes nanoporous silicon as a promising material for use in the solar cell technology. Therefore formation of nanoporous layer on frontal surface of PS/Si solar cell with lower reflectance and larger band gap, expanding the spectral range of photosensitivity, will contribute to increasing of conversion efficiency. Moreover,formation of Si-H and Si-O bonds on silicon surfaces followed by electrochemical etching in HF-based solution will provide passivation the pore surfaces.

Thus, the room temperature fabrication only nanoporous silicon layer on frontal surface of ready silicon solar cell, instead of three-step process (texturization, antireflection layer deposition and passivation), performed at high temperatures on standard technology can essentially improve the photovoltaic parameters and decrease the cost of silicon solar cells.

The potential advantages of porous silicon in silicon solar cells include:

(1) Use as antireflection coating due to a lowering of the reflectance in the sensitivity range of silicon solar cell and possibility of formation PS layer with smooth change the refractive index between those Si and air

(2) Use as a wide-band optical window (the band gap shifts from 1.1 eV to 1.9 eV as the porosity is increased from 30 to 85% [29,31] that can broad the photosensitive region of the solar cell

(3) Use as front semiconductor layer with a variable band gap that can result in increase of photocurrent

(4) Possibility of the conversion of high energy ultra-violet and blue part of the solar spectrum into long wavelength radiations due to photoluminescence in nanocrystalline porous silicon

(5) Surface passivation and gettering role of porous silicon [32]

(6) Simplicity and lower cost fabrication technology of nanoporous silicon due to electrochemical modification of silicon

The theoretical requirements for the design of single- and double-layer porous silicon as antireflection coating on silicon solar cells are given in [33]. It is shown that the effective reflectance of $(n^+\text{-}p)$Si solar cell with shallow n^+-emitter depth (about 0.3 μm) can be reduced to 7.3% with a single porous silicon layer (of 80-90 nm thickness) formed a few seconds under current density of 50 mA/cm^2. Taking account of the possibility to modulate optical properties of porous silicon by changing the electrochemical parameters during formation (dura-

http://dx.doi.org/10.5772/51593

tion of etching, current density etc.) to reduce the reflectance, structural parameters of double-layers porous silicon are calculated and lower reflectance double-layer porous silicon ARC is realized in [33]. The lowest value of the effective reflectance (below 3%) of a double-layer PS ARC on *(n^+-p)* Si cell with 0.5 μm-thick emitter have been obtained under 1 mA/cm^2 for 1 s (bottom layer of 47 nm thickness and 37% porosity) and under 50 mA/cm^2 for 100 s (top layer of 77 nm thickness and 71% porosity). It is experimentally shown that multiple PS layers ARCs can be formed in a single step procedure by changing the current density during its electrochemical preparation.

The significant reducing of the effective reflectance (up to 3%) was observed for monocrystalline silicon with porous silicon layer formed on previously texturized surface of sample [34]. Porous silicon layer was fabricated by electrochemical or chemical etch (stain etching) in HF:HNO_3:H_2O for 3-60 s on *p*-type monocrystalline silicon (Cz) or multicrystalline silicon samples. The monocrystallne wafers were previously texturised by anisotropic etching in alkaline solution.

Data of integral reflectance (for λ = 650 nm) of silicon samples without and with texturized layer, porous silicon layer or antireflection layer are presented in Table 2. The main conclusion which can be made from Table 2 is the effective reflectance for silicon samples with porous silicon layer is significantly smaller than that for samples without porous silicon layer. Moreover, the minimal effective reflectance (about of 3 %) is reached for porous silicon layer formed on previously texturized surface of silicon. The efficiency of PS/(n^+-*p*)Si solar cell with PS formed after phosphorus diffusion (12.1%) is larger compared to reference silicon solar cell without PS layer (9.4%).

Samples	Effective reflectance (%)
Polished surface	33.9
mc-Si with ARC (SnO_x)	9.4
PS by stain etching (mc-Si)	6.6
Texturisation by alkaline etching (Cz-Si)	12.6
Texturisation by alkaline etching + PS by electrochemical etching (Cz-Si)	3.4
Texturisation by alkaline etching + PS by stain etching (Cz-Si)	3.1
PS by electrochemical etching (Cz-Si polish surface)	9.7

Table 2. The effective reflectance for different silicon surfaces [34].

The porous silicon layer formed on the textured surface of crystalline silicon by using silicon-dissolved tetramethylammonium hydroxides (TMAH) method results in significant decrease of reflectance [35]. Formation of porous silicon on textured surface of silicon allowed reduce reflectance up to 5% over spectral region from 400 to 1020 nm as compared to that for textured surface without porous silicon (about 15 %). In addition, a slight increase of the effective carrier lifetime is also observed for samples with porous silicon layer.

Antireflection properties of nanoporous silicon layer on *p*-type silicon were investigated in [36]. PS layers were prepared by electrochemical etching of silicon in 1HF: $1C_2H_5OH$ solution. The average reflectance between wavelengths 300-1000 nm was 10.3 % for the optimal PS layer. The analysis of the internal quantum efficiency of *(n^+-p)* silicon solar cell with porous silicon layer as antireflection coating showed that quantum efficiency was comparable to that of a solar cell with a SiN_x antireflection coating prepared using plasma-enhanced chemical vapour deposition.

There are two technology of formation of porous silicon layer on silicon solar cells: (1) the thin porous silicon is formed on final step on surface of ready Si solar cell with metal contacts and (2) the relatively thick porous silicon layer is formed prior to emitter diffusion and metal contact deposition. In the first case the thickness of porous layer (70-150 nm) must be less than depth of n^+-p (or p^+-n)-junction (300-800 nm), $d_{PS} < d_{pn}$ and duration of electrochemical etching is short (about 5-15 s). In the second case the thickness of the porous layer (5-15μm) is significantly large than the depth of location of n^+-p (or p^+-n) junction ($d_{PS}>d_{pn}$) and duration formation of porous layer is significantly larger (about 10-30 min). It can be expected that the profile of n^+-p junction must be a flat in the first case and non-flat (it is similar to profile of porous layer surface) in the second case.

At first bellow will be considered results on photovoltaic properties of silicon solar cells with thin porous layer formed on final step fabrication of cells.

The surface modification of silicon solar cells was used for improvement of photovoltaic characteristics of silicon solar cells in [37]. *p*-type boron-doped monocrystalline silicon wafers with orientation of (100), resistivity about of 3 Ω cm and thickness of 250-380 μm were used for fabrication of solar cells by screen-printed process [8, 38]. n^+-emitter layer with 0.5-1.0 μm thickness and 15-20 Ω/□ sheet resistance was formed as a result of phosphorus diffusion. Formation of porous silicon layer on n^+-surface of the device was performed on the final step of the solar cell fabrication sequence. Fabrication of PS layer on n^+-p junction was carried out at galvanostatic condition (constant current) in an electrolyte solution $HF:C_2H_5OH:H_2O$ (1:1:1 in volume) under illumination. Choice of optimal thickness of porous silicon layer as ARC on surface of (n^+-p) silicon solar cell and choice of the refractive index, which strongly depends on porosity (see Figure 9), were defined from conditions presented above.

If conditions (8) and (9) for air/ARC/Si system are to be satisfied (n_0=1 for air and n_{Si}=3.84 for Si), then the optimal values of refractive index and thickness (a quarter of wavelength) of the porous silicon layer, acting as ARC must be (for λ= 650 nm) n_{arc}=1.96 and d_{arc}=83 nm, respectively. Taking into account the refractive index depends on porosity of porous silicon (Figure 9) one may conclude that the porous silicon layer of 80-90 nm thickness and about 55% porosity (n=2) may act as ARC having minimum reflectance, that in turn will improve the photovoltaic parameters of PS/(n^+-p)Si solar cells.

The growth rate of porous silicon on Si substrate, measured in this run for a current density of 60 mA/cm^2, was about 8 nm/s. Therefore, the time of electrochemical etching under a constant current of 40, 50 or 60 mA/cm^2 was 8-15 seconds. As a result, a blue colored PS layer between the grid fingers on the surface of the n^+-emitter silicon solar cell has been obtained. For some measurements, the PS layers were then detached from the Si substrate by electropolishing process [30]. Free-standing PS layers were characterized by porosity, thickness, re-

http://dx.doi.org/10.5772/51593

sistivity, photoluminescence and reflectance measurements. Resistivity measurements, carried out by the Van der Pauw technique on the free-standing porous silicon layer of 60% porosity, gave $3x10^4$ Ω cm.

A SEM micrograph of the front PS surface obtained by using scanning electron microscopy (SEM) (JSM-5410LV) is shown in Figure 12. Cross cut representation of silicon layer showed that the pores have a conical form.

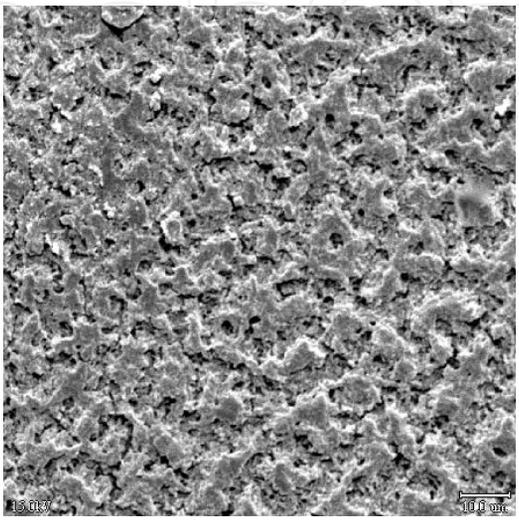

Figure 12. Scanning electron microscopy of porous silicon layer surface.

Figure 13 shows the photoluminescence spectrum of the PS layer (60% porosity) on Si substrate, where the spectrum illustrates the peak at λ=580 nm (the orange region of the solar spectrum). Measurements of distribution of photoluminescence intensity along the thickness of the PS layer (of thickness 10 μm) showed that the intensity approximately linearly decreasesfrom the surface deep down. Similar results were also obtained by investigations of samples with PS layers of different thicknesses. Observation of photoluminescence in PS at visible region of the spectrum can be interpreted by quantum confinement effect causing the confinement of the charge carriers in nanocrystalline silicon wall separating the pore [39].

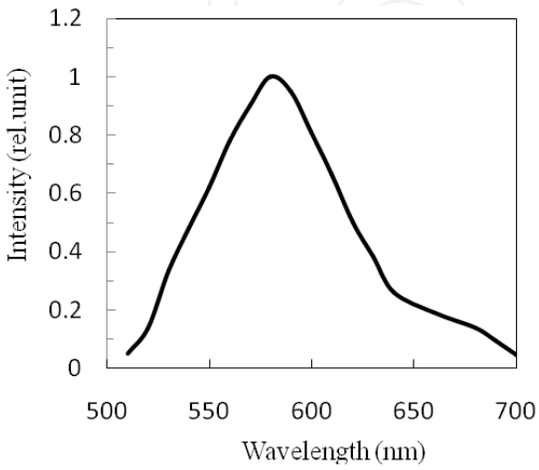

Figure 13. The photoluminescence spectrum for porous silicon layer.

The integrated reflectance spectra of the polished silicon surface before and after porous silicon layer (of 60% porosity) formation showed the significant lowering of the reflectance (to 4%) as compared to polished silicon (about 38-45%). These data show that PS on (n^+-p) silicon solar cell can be used as effective antireflection coating.

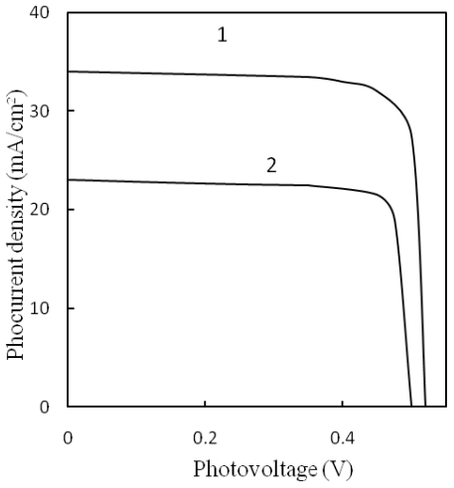

Figure 14. Photocurrent density-voltage chracteristics of (n^+-p) silicon solar cell (1) with and (2) without PS layer.

The current-voltage characteristics of n^+-p silicon solar cells without and with porous silicon layer of 60% porosity ((n^+-p)Si and PS/(n^+-p)Si structures respectively), measured under AM1.5 illumination, have been presented in Figure 14. As a result, due to the PS coating, the short-circuit current density increased from 23.1 to 34.2 mA/cm^2 and the open-circuit voltage increased from 500 to 520 mV. The experimental results on the photovoltaic parameters for thirty solar cells before and after formation of the PS layer on n^+-emitter surface showed that the mean increment of photocurrent density is about 48% (Table 3). At the same time, the open-circuit voltage increase is about 4%. The fill factor remains approximately the same for cells with porous layer (FF=0.75) as compared to the solar cells without porous layer (FF=0.74). The mean efficiency of photovoltaic conversion for solar cells with PS layer increased from 12.1 to 14.5%, what equals a relative increment of about 20%.

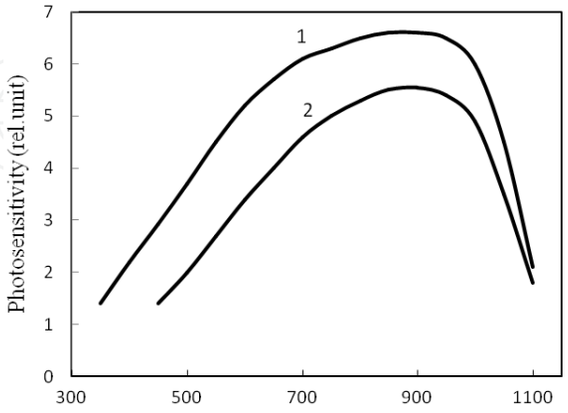

Figure 15. The photosensitivity spectra of (1) PS/(n^+-p)Si and (2) (n^+-p) Si solar cells.

The photosensitivity spectra of the solar cells with and without PS layer were presented in Figure 15. The value of photosensitivity for the PS/(n^+-p)Si cell is larger (by about 25%) and

http://dx.doi.org/10.5772/51593

the spectral photosensitivity region is considerably wider than those for (n^+-p) Si cell without the PS layer. The significant improvement of photovoltaic characteristics of the PS/(n^+-p)Si solar cell was attributed mainly to the two-fold role of the porous silicon layer on surface of the n^+-emitter. Firstly, it behaves as a antireflection coating, increasing the incident photon flow on the p^+-n junction and secondly, it plays the role of a wide-band gap optical window (about of 1.8-1.9eV for PS of 60% porosity), broadening the spectral region of photosensitivity of the cell to the ultraviolet part of solar spectrum.

Solar cell	J_{sc} (mA/cm^2) or I (mA)	V_{oc} (mV)	FF	Eff. (%)	Reflectance (λ=650 nm)	Reference
(n^+-p) Si	23.1	500	0.74	12.1	28	[37]
PS/(n^+-p) Si	34.2	520	0.75	14.5	4	
(n^+-p) Si	21.5	580	0.55	7.5	12	[40]
PS/(n^+-p) Si	28.4	585	0.74	12.5	3	
(n^+-p) Si	95 mA	580		10.3		[41]
PS/(n^+-p) Si	137 mA	570		13.5		
(n^+-p) Si	17.2	598	0.74	7.6	7	[42]
PS/(n^+-p) Si	20.1	606	0.75	9.5	12	
Text. (n^+-p) Si	23.3	592	0.70	9.6	3	
PS/Text. (n^+-p) Si	25.5	595	0.74	11.2		
(n^+-p) Si	18.5	580	0.73	7.85	7	[43]
PS/(n^+-p) Si	27.2	601	0.77	12.54		
PS/ (n^+-p) Si	33.4	460			9	[44]
SiO_x/(n^+-p) Si	34.8	530			3.8	
(p^+-n)PS/Si (100)	15.9 mA	480	0.81	15.4	7	[45]
(p^+-n)PS/Si (111)	12.4 mA	440	0.82	11.2	16	
(n^+-p)PS/Si (111)	12.4 mA	440	0.82	11.2		[47]
SiO_2/(n^+-p)Si (111)	6.04 mA	370	0.79	4.4		
(ZnO-TiO_2)/(n^+-p)Si	10.2 mA	410	0.81	8.4		
(p^+-n)PS/Si PS on one side	8.8 mA	430	0.78	7.4	16	[48]
(p^+-n)PS/Si/PS PS on both sides	12.4 mA	490	0.84	12.75	6	
(n^+-p)PS/Si	28.9	627	0.76	13.8	9	[49]
PS/(n^+-p) Si	26.3	602	0.76	12	10	[50]
SiN/(n^+-p) Si	28.4	606	0.75	13		
(n^+-p) mc-Si	26.6	572	0.75	11.3	15	[51]
PS/ (n^+-p) mc-Si	28.9	582	0.76	12.7	5	
(n^+-p) mc-Si	29.8	577	0.5	12.9	8	[7]
(n^+-p)PS/mc-Si	30.2	587	0.76	13.5		

Table 3. Photovoltaic parameters of silicon solar cells without and with porous silicon layer.

Change the porosity deep down to PS layer can also stimulates the improvement of the photovoltaic parameters of solar cells. Experimentally observed decrease of intensity of the photoluminescence peak at 580 nm deep down to PS layer, which consists of pores of conical form, can be circumstantial evidence for decrease of porosity deep down. Taking into account that the band gap energy of nanoporous silicon increases with increment of porosity due to quantum confinement of carrier charges (see Figure 11), one can assume that the porous silicon layer on the (n^+-p)Si cell is a semiconductor with variable band gap width (changing from about 1.8-2.0 eV on the front PS surface to 1.1 eV on the PS/n^+Si interface). As a result, the internal electrical field of the porous layer with variable band gap can also increase of the photocurrent generated in the PS/(n^+-p)Si solar cell.

The original formation technique of porous silicon layer on silicon solar cells was used in [40]. n^+-p junctions were obtained by phosphorus diffusion into monocrystallinep-type silicon wafers. PS layer was formed after deposition of front grid contact. New method PS layer formation consisted in deposition a thin Al film on front surface silicon cell and then HF-spray-etching. Advantage of method is use HF solution only, instead HF:HNO_3 composition, since HF-spray-etching does not influence on front grid metallic contact. Hydrogen-rich PS prepared by HF-spray-etching method plays role of a passivation layer and decreases the surface reflectance from 12% for textured surface to 3% for textured surface in the presence of a thin porous silicon layer. Formation of PS layer prepared under optimized HF-spraying conditions improves the conversion efficiency from 7.5 to 12.5% (Table 3). The observed results were discussed throughout increase of light absorption due to reflectance lowering and band gap widening. Unfortunately, data on thickness, porosity and other parameters of porous layers are not presented in [40].

The porous silicon as ARC in (n^+-p) silicon solar cells was used in [41]. Thin porous silicon layer (of thickness about 100 nm) on n^+-emitter was formed on final stage of (n^+-p) solar cell fabrication. 1HF : 1C_2H_5OH and 1HF : 1C_2H_5OH : H_2O solutions were used as electrolyte during anodization modification of silicon (for 3-12 s). n^+-p junction with n^+-emitter of 400 nm thickness was formed by phosphorus diffusion in monocrystalline p-type (100) silicon of 1.5 Ω cm resistivity.The reflection spectra of porous layer prepared on the polished surface of n^+-emitter showed that the average reflectance is about 7.6% in the wavelength range 400-700 nm with minimum value of 1.4% at 580 nm. The photovoltaic parameters of (n^+-p)Si solar cells before and after formation of PS layer are presented in Table 3. It is seen that the efficiency of solar cell increased from 10.3 to 13.5% as result of fabrication of porous layer on front surface of the cell. The significant increasing for the short-circuit current (from 95 to 137 mA) and very small decreasing of the open-circuit voltage were observed for cells with porous silicon coating. Authors [41] supposed that the formation of porous silicon layer on silicon solar cells does not ensure necessary level of passivation and also does not have sufficient temporal stability.

The photovoltaic parameters of (n^+-p) Si solar cells with and without thin porous silicon layer prepared by standard screen-printed technique are studied in [42]. *P*-type Si (100) wafers of 1.5 Ω cm resistivity and 20 cm^2 surface were used. Formation of porous silicon layer on n $^+$-surface of cells was performed by electrolytic anodization in 1HF: 4C_2H_5OH solution with

a current density of 10 mA/cm^2 during short time 10 s. Data on characteristics of solar cells, prepared on base of polished monocrystalline and textured monocrystalline silicon without and with porous layer are presented in Table 3. The main conclusion from results presented in Table 3 consists in increasingthe short-circuit current density and efficiency of silicon solar cells with porous layer. For both group cells prepared on polished and textured silicon with porous layer efficiency increases by about 20-25% compared to a cells without porous silicon layer. However the open-circuit voltage and fill factor for cells with porous layer remain almost same with those for cells without porous silicon. The minimum reflectance and the best photovoltaic parameters have the solar cells with porous silicon layer prepared on textured surface.

A significant improvement in efficiency of (n^+-p) Si solar cells with the thin porous silicon layer has been achieved in [43]. Float-zone (100) oriented p-type silicon with 1Ω cm resistance was used as starting material. Formation of the porous silicon layer was made on finished solar cell during chemical etching in HF: HNO_3:H_20 solution for 20 s. The reflectance of polished Si sample is significantly lowered after porous layer formation from 36 to 9.5%.The silicon solar cell with porous layer leads to a 46% and 38% relative improvement in photocurrent density and efficiency respectively (Table 3). The observed enhancement in the photovoltaic parameters was attributed to both the antireflection and passivation properties of porous silicon. The passivation capabilities of PS accompanied with lowering of recombination velocity of charge that can arise from the presence of Si-hydrides and Si-hydroxides on pore surfaces.

Double layers SiO_x/PS structure as antireflection coating in (n^+-p) Si solar cells prepared the screen-printing technique was studied in [44]. Then porous silicon layers were fabricated on the front surface of screen-printing (n^+-p) Si solar cells by electrochemical etching in 1HF: $3C_2H_5OH$ solution at a current density of 20 mA/cm^2 for 4-12 s. The silicon oxide films of different thickness (70-105 nm) were deposited on porous silicon by PECVD method. Decrease of reflectance and improvement of photovoltaic parameters of double layer SiO_x/PS/(n^+-p) Si cells were received compared to the single PS/(n^+-p) Si cells. Best results were obtained when the thickness of SiO_x film and PS layer (P=60%) are 105 and 60 nm respectively (Table 3). An improvement in the open-circuit voltage of 14% for double-layer ARC authors [44] attribute to enhancing the surface passivation of the pores due to diffusion of hydrogen from SiO_x film.

There are a number of studies on silicon solar cells with thick porous silicon coating in which the porous layer is formed before fabrication of n^+-p (or p^+-n) junction.

The orientation of porous silicon influences of performance of silicon solar cells [45]. (p^+-n) silicon solar cells were prepared on base of n-type Si of (111) and (100) orientation (0.75 Ω cm). p^+-type doping was achieved by boron diffusion. Porous silicon layer on p^+-silicon was fabricated by electrochemical anodization in 1HF: $3C_2H_5OH$ solution at a current density of 50 mA/cm^2 for 20 min. The surface reflectance of porous silicon on (100) Si is significantly less (8 %) than that for (111) Si (16%). The photovoltaic parameters for (100) Si and (111) Si-based solar cells presented in Table 3 show that the conversion efficiency of (100) Si-based cells is larger (15.42%) than that of (111) Si-based cells (12.4%). The observed results authors

explain formation higher pyramids on (100) Si surface compared to (111) Si surface that results in lower reflectance.

It is to be noted that for thick porous silicon layer when it thickness is larger than that of p^+*(or* n^+*)*-emitter, non-uniformity of p^+-n (or n^+-p) junction profile can make worse the parameters of cells. Influence of different PS layer thickness on photovoltaic properties of n^+-p silicon solar cells showed that both external and internal quantum efficiencies are improved as far as PS/Si interface does not overpass the n^+-p junction [46]. It can mean that when the thickness of PS layer is larger than that of n^+emitter region, i.e. the space-charge region locates in PS layer, the surface defects of PS layer stimulate the increase the recombination rate of photocarriers.

The comparative investigations of (n^+-p) Si (111) solar cells with single layer ARC (SiO_2), double layers ARC (ZnO/TiO_2) and the porous silicon layer are carried out in [47]. The porous silicon layers were formed on phosphorus-doped n^+-layer of solar cells in 1HF: $3C_2H_5OH$ solution at current density 60 mA/cm^2 for 30 min. The best photovoltaic characteristics showed the silicon solar cells with porous layer (see Table 3). From SEM micrograph presented in the work it is seen that thickness of porous silicon is significantly larger than the depth of p^+-n junction in silicon. It can make worse the characteristics of the p^+-n cells.

Above we considered the results of studies on silicon solar cells with porous layer formed only on front side of cell. Interesting data for silicon solar cells with porous layers prepared *on both sides of the (111) n-type Si wafers* (of 0.75 Ω cm resistivity and of 283 μm thickness) are given in [48]. The porous silicon layers on the polished front side and the unpolished backside were obtained by electrochemical process in 1HF : 4 C_2H_5OH solution under 60 mA/cm^2 for 15 min for each side (before boron diffusion and metal contact deposition). SEM images showed that the porous surface formed on the front polished side has discrete pores, whereas the porous silicon surface created on unpolished backside is shaped in small pores which are attributed to an increase in surface roughness. The reflectance of the PS front and back sides in the spectral range 400-1000 nm are about 16% and 6% respectively. As is seen from Table 3 the efficiency of (p^+-n)PS/nSi/PS solar cell with PS layer on both sides of Si is increased to 12.75% compared to solar cell with PS layer on the unpolished side (7.4%).

The formation of PS layer during the normal cleaning sequence at the beginning of the solar cell process was carried out in [49]. Porous silicon layers on p-type silicon wafer prepared by stain etching in HF:HNO_3 showed reflectance as low as 9 %. Photovoltaic characteristics of the best porous silicon cells fabricated by screen-printed technique are given in Table 3. The high values of photovoltaic parameters of (n^+-p)PS/pSi solar cells are attributed to lower reflectance and passivation properties of PS layer.

Thin porous silicon layer formed on dendritic web and string ribbon silicon by chemical etching in HF:HNO_3:H_2O solution for a few seconds increases the lifetime of the minority carriers by a factor 3.3 [50]. The additional heat treatment (860°C, 2 min) or simultaneous phosphorus and aluminum diffusion after PS layer formation results in lifetime enhancement by a factor 8.3 or 5.8 respectively. In opinion of authors [50] porous silicon induced lifetime enhancement can be caused by the gettering properties of PS layer. Photovoltaic

characteristics of (n^+-p) silicon solar cells with porous silicon layer and SiN antireflection coating are given in Table 3. It is seen that both type solar cells have almost same parameters.

The improvement of photovoltaic parameters of *multicrystalline*(n^+-p) Si solar cells with porous silicon layer is observed in [51]. Formation of porous silicon layer on textured surface of p-type mc-Si (1Ω cm) was performed by two-step chemical etching of silicon before phosphorus diffusion. It is shown that macroporous silicon layer formed before phosphorus diffusion results in texturisation of mc-Si with the larger angle than that obtained classical texturisation based in KOH. The surface reflectance of mc-Si with PS layer with phosphorus glass drops up to 5% compared to that for mc-Si with phosphorus silica glass but without PS layer (16%). The main parameters of (n^+-p) mc-Si based solar cells (of 25 cm^2 size) without and with PS layer were presented in Table 3. Formation of PS layer on mc-Si allows enhance the efficiency up to 12.7% that is close the efficiency limit of the mc-Si solar cells with TiO_x antireflection coating. Additional etching of (n^+-p) mc-Si solar cell in $98HNO_3$:2HF solution for 300 s (after PS formation) improves its photovoltaic parameters [7] (see Table 3).

Gettering behavior of PS layer on silicon leading to enhancement of the lifetime of the non-equilibrium minority carriers and improvement of silicon solar cell characteristics have been considered in [52-54]. The porous silicon containing a large number of small pores with diameter between 4-50 nm shows very large the surface area-to-volume ratio (about of 500 cm^2/m^3). The extremely large pore surfaces and their very chemical activity ensure possibilityof application related with gettering of impurities and defects. The high-temperature annealing of the chemical etched porous silicon surface can enhance the impurity diffusion into the porous silicon network and thereby acting as an efficient external gettering site. The oxidation rate of porous silicon due to its mesapore structure is significantly larger (by 10-20 times) than that for single-crystalline silicon surface [52]. Gettering by porous silicon consists of oxidizing the porous silicon layer in wet oxygen ambient condition followed by the removal oxide in a dilute HF solution. The lattice mismatch between porous layer and silicon substrate can stimulate the gettering of impurities and defects.

The gettering-induced enhancement in the minority carrier diffusion length in multicrystalline silicon (mc-Si) with porous silicon layer on its surface was studied in [53]. The PS/Si/Al structures prepared by formation of porous layer in front surface of silicon and by vacuum evaporation of aluminum layer (2 μm) on the other side of sample were exposed to the wet oxidation of the porous silicon (950°C). Measurements showed that the minority carrier diffusion length for Si in such structure (about 190 nm) is larger than that for reference Si sample (about 100 nm). Co-gettering effect for PS/Si/Al consists in out-diffusion of impurities throughout the porous silicon layer and the aluminum. For {phosphorus layer/silicon/aluminum layer} structures (without porous layer) usually used for fabrication of silicon solar cell influence of co-gettering on the diffusion length of minority carriers is less (about 100 nm).

The PS/Si/Si structures prepared by forming porous silicon layers on both sides of Si wafer and then coated with phosphorus dopant ($POCl_3$) and heat treated at 900°C for 90 min discovered the improvement of the electrical and recombination characteristics of silicon [54]. Diffusion of phosphorus into PS layer is accompanied by gettering of eventual impurities towards the phosphorus doped PS layer. As a result of removal of impurities, increasing the

mobility of the majority carriers and the diffusion length of minority carriers are observed. Removal of eventual impurities and defects away from the device active regions allowed to improve output characteristics of silicon solar cells.

Above, the results of influence of the porous silicon as an active element in thick crystalline silicon solar cells have been considered. It is shown the porous silicon as antireflection coating significantly improves the performance of silicon solar cells. In last year's porous silicon layer were also used as sacrificial layer for fabrication of thin-film silicon solar cells. As known the monocrystalline silicon which intensively are used in commercial solar cell applications is high cost material. The reduction in the amount of high-quality expensive silicon material per solar cell is one of ways of lowering the cell coat. At present one of the technologies developed to fulfill the aim of reduction the cost of silicon solar cell is porous silicon (PSI)-transfer process [55]. The thickness of monocrystalline silicon solar cell prepared by PSI-process (about 5-50 μm) is significantly lower than that of crystalline silicon cell fabricated by standard technology (250-300 μm). The PSI-transfer process consists of four steps. *First*, double layers of porous silicon are fabricated by electrochemical etching on surface of monocrystalline silicon: the 1-2 μm-thickness low-porosity layer (20%) at the top and 350 nm-thickness high-porosity layer (50-60%) beneath. *Second*, thin monocrystalline silicon layer (about 5-50 μm thickness) epitaxial grows on top (low-porosity) layer. Low-porosity layer is of monocrystalline quality which allows the growth of a high quality epitaxial layer of silicon. *At third step* the epitaxial silicon layer is detached from silicon substrate through a high-porosity layer by lift-off technique and then it is transferred onto a foreign substrate. *At final step* thin-film silicon solar cell is fabricated by standard or other technology. Shortly after using of PSI-process cell efficiency gradually increased from 12.5% (in 1997) to 16.9% (in 2009). Today the record value of efficiency of 19.1% (S=4 cm^2,V_{oc}=650 mV, J_{sc}=37.8 mA/cm2, FF=0.78) for monocrystalline silicon solar cell of 43 μm thickness prepared by porous silicon transfer technique was demonstrated [56]. It should be noted that porous silicon transfer process is certainly complex for industrial application. Nevertheless it shows the high efficiency potential of the porous silicon transfer process.

6. Conclusion

The review of investigations of the use of the nanoporous silicon in silicon solar cell showed that an increase in the conversion efficiency (about of 25-30%) is achieved for PS/Si solar cell compared to a cell without a PS layer. At the same time, the performance of silicon solar cells with PS layer is more than that of silicon solar cells with conventional ARC. The lower value of effective reflectance (up to 3%) for nanoporous silicon layer that significantly reduces the optical losses is one of main reasons of improvement of performance of PS/Si solar cell. A wide-band gap nanoporous silicon (up to 1.9 eV) resulting in widening of the spectral region of photosensitivity of the cell to the ultraviolet part of solar spectrum may promote the increase the efficiency of silicon solar cells with PS layer. The internal electric field of porous silicon layer with variable band gap (due to decrease of porosity deep down) can stimulate an increase in short-circuit current (Figure 16).

http://dx.doi.org/10.5772/51593

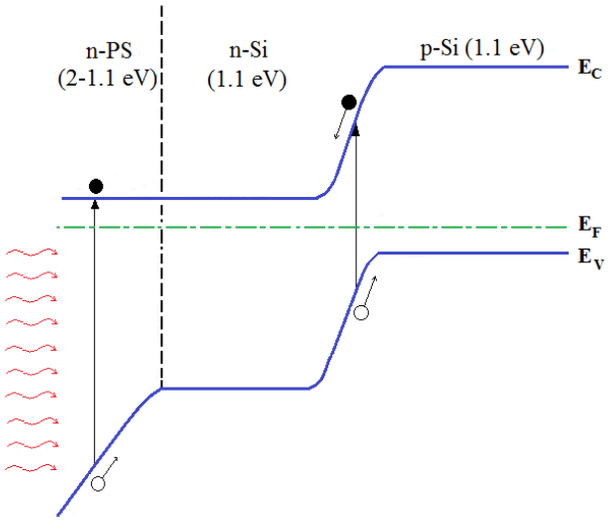

Figure 16. Energy band diagram of *n*PS/(n^+-*p*) Si solar cell.

Additionally, the intensive photoluminescence in the red-orange region of the solar spectrum observed in porous silicon under blue-light excitation can increase the concentration of photo-exited carriers. It is necessary to take into account the passivation and gettering properties of Si-H and Si-O bonds on pore surfaces which can increase the lifetime of minority carriers.

Porous silicon, along with above advantages, in some cases e.g. due to its high resistivity can reduce the output parameters of PS/Si solar cells. Contribution of resistance (about $5x10^{-2}$ Ω) of thin porous silicon layer (about 100 nm) in total series resistance of the solar cell (about 0.5-1.0 Ω) is negligible and therefore it must not influence on parameters of cells. The resistance of thick PS layer (5-15 μm) can essentially increase the total series resistance and thereby it can reduce the photovoltaic parameters of silicon solar cell. However, as is seen from Table 3 reducing of parameters of PS/Si solar cells with thick PS layer was not observed. It tentatively can be explained that formation n^+or p^+-emitter layer by phosphorus or boron diffusion in PS is accompanied with decrease of layer resistance. Moreover, the non-flatprofile of n^+-*p* (or p^+-*n*) junction in PS/Si cells with thick PS layer (prepared before junction formation) does not result in reducing of efficiency (see Table 3). Explanation of this problem demands of further investigations.

Note should be taken that properties of PS layer and thereby photovoltaic characteristics of solar cell can change on running under illumination, heating etc. At present, as far as our knowledge goes, publications on temporal stability of PS-based solar cells are almost absent in literature.Works related with degradation phenomena in PS/Si solar cells is the matter of topical interest for further researches.

Judging by the results presented in this review and taking into account the simplicity of fabrication of porous silicon layer on silicon we can safely draw to the conclusion that the nanoporous silicon is a good candidate for use on preparation of low cost silicon solar cells with high efficiency. It gives hope for the industrial production of PS-based silicon solar cells.

Author details

Tayyar Dzhafarov*

Address all correspondence to: caferov@physics.ab.az

Department of Solar and Hydrogen Cells, Institute of Physics, Azerbaijan National Academy of Sciences, Azerbaijan

References

[1] Goetzberger, A., & Hebling, C. (2000). Photovoltaic Materials, Past, Present, Future. *Solar Energy Materials and Solar Cells*, 62, 1-19.

[2] Sze, S. (1990). Physics of Semiconductor Devices. New York: John Wiley & Sons.

[3] Canham, L., editor. (1997). Properties of Porous Silicon. London: IEE-Inspec.

[4] Bisi, O., Ossicini, S., & Pavesi, L. (2000). Porous Silicon: A Quantum Sponge Structure for Silicon Based Optoelectronic. *Surface Science Reports*, 38, 1-126.

[5] Fahrenbruch, A., & Bube, R. (1983). Fundamentals of Solar Cells, New York.

[6] Gupta, S., Srivastaya, M., & Gupta, A. Mathematical Formulation Comparative Analysis of Losses in Solar Cells. http://www.tutorialspoint.com/white-papers.

[7] Lipinski, M., Panek, P., & Ciach, R. (2003). The Industrial Technology of Crystalline Silicon Solar Cells. *J. Optoelectronics and Advanced Materials*, 5, 1365-1371.

[8] Neuhaus, D., & Munzer, A. (2008). Industrial Silicon Wafer Solar Cells. *Advances in Electronics*, 4, 2-15.

[9] Moller, H. J. (1993). Semiconductor for Solar Cells. Boston: Artech House.

[10] Green, M. (1999). Limiting Efficiency of Bulk and Thin-film Silicon Solar Cells in Presence of Surface Recombination. *Progress in Photovoltaic*, 1999, 7(3), 327-330.

[11] Neizvestny, I. (2011). Nano-technologies in Solar Cells. *International Association of Academies of Sciences, Scientific Council on New Materials, conference proceedings*, October 5-7, 2011, Kiev.

[12] Born, M., & Wolf, E. (1970). Principles of Optics. London: Pergamon Press.

[13] Goodman, A. (1978). Optical Interference Method for the Approximate Determination of Refractive Index and Thickness of a Transparent Layer. *Applied Optics*, 17(17), 2779-2789.

[14] Sopori, B., & Pryor, R. (1983). Design of Antireflection Coatings for Textured Silicon Solar Cells. *Solar Cells*, 1983, 8, 249.

[15] Jayakrishnan, R. (2009). Dielectric Coating Agents for Passivation and Anti-reflection. *Photovoltaic International*, 6, 83-86.

[16] Chen, Z., Sana, P., & Salami, J. (1993). A Novel and Effective PECVD SiO_2/SiN Antireflection Coating for Si Solar Cells. *IEE Trans. Electron Device*, 40(6), 1161-1165.

[17] Mahdjoub, A. (2007). Graded Refractive Index Antireflection Coatings Based on Silicon and Titanium Oxides. *Semiconductor Physics, Quantum Electronics and Optoelectronics*, 10(1), 60-66.

[18] Feng, Z., & Tsu, R. (1994). Porous Silicon. Singapore: World Scientific.

[19] Beale, M., Uren, J., Chew, N., & Cullis, A. (1985). An Experimental and Theoretical Study of the Formation and Microstructure of Porous Silicon. *Journal of Crystal Growth*, 73, 622-636.

[20] Remache, L., Mahdjoub, A., Fourmond, E., Dupuis, J., & Lemiti, M. (2010). Design of Porous Silicon/PECVD SiO_xAntireflection Coatings for Silicon Solar Cells. *Intern. Conference on Renewable Energies and Power Quality (ICREPQ-2010)*, Granada, Spain, 23-25 March.

[21] Dzhafarov, T. D., & Can, B. (2000). The Diffusion Distribution of Hydrogen and Oxygen in Porous Silicon Films. *Journal of Materials Science Letters*, 19, 287-289.

[22] Abdullaev, G. B., & Dzhafarov, T. D. (1987). Atomic Diffusion in Semiconductor Structures. New York: Harwood Academic Press.

[23] Dzhafarov, T., & Aydin, S. (2010). Diffusion of Hydrogen in Porous Silicon-based Sensors. *Journal of Porous Media*, 13(2), 97-102.

[24] Cisneros, R., Pfeiffer, H., & Wang, C. (2010). Oxygen Absorption in Free-Standing Porous silicon: A Structural, Optical and Kinetic Analysis. *Nanoscale Res. Lett.*, 5(4), 686-691.

[25] Barla, K., Herino, R., Bomchil, G., Pfister, J., & Freund, A. (1984). Determination of Lattice Parameters and Elastic Properties of Porous Silicon by X-ray Diffraction. *Journal of Crystal Growth*, 8, 727-732.

[26] Barla, K., Herino, R., Bomchil, G., Pfister, J., & Baruchel, J. (1984). X-ray Topographic Characterization of Porous Silicon Layers. *Journal of Crystal Growth*, 68, 721-726.

[27] Bellet, D., & Dolino, G. X. (1996). X-Ray Diffraction Studies of Porous Silicon. *Thin Solid Films*, 276(1), 778-782.

[28] Perez, E. (2010). Design, Fabrication and Characterization of Porous Silicon Multilayer Optical Devices. Ph.D. thesis, Universitet Rovirai Virdali.

[29] Dzhafarov, T., & Aydin, S. (2009). Nano-Porous Silicon for Gas Sensors and Fuel Cells Applications. *Journal of Qafqaz University*, 25, 20-35.

[30] Dzhafatov, T., Oruc, C., & Aydin, S. (2004). Humidity-Voltaic Characteristics of Au-Porous Silicon Interfaces. *Journal of Physics D: Applied Physics*, 37, 404-408.

[31] Pickering, C., Beale, M., Robbins, D., Pearson, R., & Greef, R. (1984). Optical Studies of the Structure of Porous Silicon Films Formed in p-type Degenerate and Non-degenerate Silicon. *J. Phys. C*, 17, 6535-6552.

[32] Schirone, L., Sotgiu, G., Montecchi, M., & Parisini, A. (1997). Porous Silicon in High Efficiency Large Area Solar Cells. *Conference proceedings, Progr.14 European PV Solar Energy Conf.*, Barcelona, Spain, 1479-1482.

[33] Strehlke, S., Bastide, S., Guillet, J., & Levy-Clement, J. (2000). Design of Porous Silicon Antireflection Coatings for Silicon Solar Cells. *Materials Science and Engineering*, B69-70, 81-86.

[34] Lipinski, M., Panek, P., Beilanska, E., Weglowska, J., & Czternastek, H. (2000). Influence of Porous Silicon on Parameters of Silicon Solar Cells. *Opto-Electronics Review*, 8(4), 418-420.

[35] Weiying, O., Lei, Z., Hongwei, D., Jun, Z., & Wenjing, W. (2011). Optical and Electrical Properties of Porous Silicon Layer Formed on the Textured Surface by Electrochemical Etching. *Journal of Electronics*, 32(5), 1-5.

[36] Kim, J. (2007). Formation of a Porous Silicon Antireflection Layer for a Silicon Solar Cell. *Journal of Korean Physical Society*, 50(4), 1168-1171.

[37] Dzhafarov, T., Aslanov, S., Ragimov, S., Sadigov, M., & Aydin Yuksel, S. (2012). Effect of Nanoporous Silicon Coating on Silicon Solar Cell Performance. *Vacuum*, 86(12), 1875-1879.

[38] Green, M. (1999). Limiting Efficiency of Bulk and Thin-film Silicon Solar Cells in the Presence of Surface Recombination. *Progress in Photovoltaic*, 7, 327-338.

[39] Canham, L. (1990). Silicon Quantum Wire Array Fabrication by Electrochemical and Chemical Dissolution of Wafers. *Appl. Phys. Lett.*, 57, 1046.

[40] Saadoun, M., Ezzaaoia, H., Bassais, B., Boujmil, M., & Bennaceur, R. (1999). Formation of Porous Silicon for Large-area Silicon Solar cells: A New Method. *Solar Energy Materials and Solar Cells*, 59, 377-385.

[41] Yerokhov, V., Melnik, I., Tsisaruk, A., & Semochko, I. (2000). Porous Silicon in Solar Cell Structures. *Opto-Electronics Review*, 8(4), 414-417.

[42] Panek, P., Lipinski, M., & Czternastek, H. (2000). Porous Silicon Layer as Antireflection Coating in Solar Cells. *Opto-Electronics Review*, 8(1), 57-59.

[43] Chaoui, R., & Messaoud, A. (2007). Screen-Printed Solar Cells with Simultaneous Formation of Porous Silicon Selective Emitter and Antireflection Coating. *Desalination*, 209, 118-121.

[44] Remache, L., Mahdjoub, A., Fourmond, E., Dupuis, J., & Lemiti, M. (2010). Design of porous silicon/PECVD SiO_x antireflection coatings for silicon solar cells. *International Conference on Renewable Energies and Power Quality (ICREPQ-2010)*, 23-25 March, Granada.

[45] Aziz, W., Ramizy, A., Ibrahim, K., Omar, K., & Hassan, Z. (2009). Effect the Orientation of Porous Silicon on Solar Cell Performance. *Optoelectronics and Advances Materials*, 3(12), 1368-1370.

[46] Bastide, S., Albu-Yaron, A., Strehlke, S., & Levy-Clement, C. (1999). *Formation and Characterization of Porous Silicon Layers for Application in Multicrystalline Silicon Solar Cells*, 57, 393-417.

[47] Ramizy, A., Aziz, W., Hasan, Z., Omar, K., & Ibragim, K. (2000). The Effect of Porosity on the Properties of Silicon Solar Cells. *Microelectronic International*, 27(2), 117-120.

[48] Ramizy, A., Hassan, Z., Omar, K., Al-Douri, Y., & Mahdi, M. (2001). New Optical Features to Enhance Solar Cell Performance Based on Porous Silicon Surfaces. *Applied Surface Science*, 257, 6112-6117.

[49] Ludemann, R., Damiani, B., & Rohatgi, A. (2000). Novel Processing of Solar Cells with Porous Silicon Texturing. *In: Proceedings of the 28-th IEEE Photovoltaic Specialists Conference*, 15-22 September, Anchorage, Alaska, 299-301.

[50] Hilali, M., Damiani, B., & Rohatgi, A. Lifetime Enhancement During Processing of Porous Silicon Cells. http://smartech.gatech.edu/jspui/bitstream.

[51] Panek, P. (2004). Effect of Macroporous Silicon Layer on Opto-Electrical Parameters of Multicrystalline Silicon Solar Cells. *Opto-Electronics Review*, 12(1), 45-48.

[52] Hirscheman, K., Tsybeskov, L., Duttagupta, S., & Fauchet, P. (1996). Silicon-based Visible Light-Emitting Devices Integrated into Microelectronic Circuits. *Nature*, 384, 338-340.

[53] Vinod, P. (2007). Porous Silicon and Aluminum Co-gettering Experiment in p-Type Multicrystalline Silicon Substrates. *Science and Technology of Advanced Materials*, 8, 231-236.

[54] Khedher, N., Hajji, M., Ben Jaballah, A., & Quertani, B. (2005). Gettering of Impurities from Crystalline Silicon by Phosphorus Diffusion Using a Porous Silicon Layer. *Solar Energy Materials & Solar Cells*, 87(1-4), 605-611.

[55] Solanski, C., Bilyalov, R., Poortmans, J., Nijs, J., & Mertens, R. (2004). Porous Silicon Layer Transfer Processes for Solar Cells. *Solar Energy Materials and Solar Cells*, 83, 101-113.

[56] Petermann, H., Zielke, D., Schmidt, J., Haase, F., Rojas, E., & Brendel, R. (2012). Efficient and 43μm-Thick Crystalline Si Solar Cell from Layer Transfer Using Porous Silicon. *Progress in Photovoltaic: Research and Application*, 20(4), 1-5.

IntechOpen